UNITED NATIONS UNIVERSITY
UNU-LRT
Land Restoration Training Programme
Keldnaholt, 112 Reykjavik, Iceland

Final project 2017

ASSESSING DESERTIFICATION AND LAND DEGRADATION USING TRENDS OF NORMALIZED DIFFERENCE VEGETATION INDEX TIME SERIES: CASE STUDY IN STEPPE ZONE IN MONGOLIA

Ikhbayar Tsevelmaa
Agency for Land Administration and Management, Geodesy and Cartography
Government Building 12, Ulaanbaatar, Mongolia
tikhbayr@yahoo.com

Supervisors:
Atli Gudjónsson
EFLA Engineering
atli.gudjonsson@efla.is

Ingibjörg Jónsdóttir
University of Iceland
ij@hi.is

ABSTRACT

Desertification and land degradation are causing a serious environmental problem in Mongolia, with climate change and human activities being major contributors to the land degradation. This study was aimed to assess land degradation and desertification using the remotely sensed Normalized Difference Vegetation Index (NDVI) time series and the amount of precipitation. GIS and statistical analyses were used to estimate the trend of the annual average NDVI for June, July and August from 2006 to 2016. Moreover, analyses were conducted to identify the effects of precipitation variation and human activities on the trend of NDVI. The Mongolian real steppe subzone was selected as a study site since the area is vulnerable to desertification. The study results reveal an increasing trend in NDVI values in 86.54% of the total study area and a decreasing trend in NDVI values in 13.5% from 2006 to 2016. Overall, 13.5% of the total area, or a 2,923.4 sq. km area, has been affected by desertification. The human impact zone had a higher declining trend than the no impact zone. There was a positive moderate correlation between change in precipitation and the NDVI trend in the study area. The study indicates that the effects of precipitation variance on the changes in the trend of the NDVI resulted from more than human activities in the study area.

This paper should be cited as:
Tsevelmaa I (2017) Assessing desertification and land degradation using trends of Normalized Difference Vegetation Index time series: case study in steppe zone in Mongolia. United Nations University Land Restoration Training Programme [final project]
http://www.unulrt.is/static/fellows/document/tsevelmaa2017.pdf

TABLE OF CONTENTS

1. INTRODUCTION

Mongolia is a Central Asian land-locked country located between Russia and China and its territory covers 1,566,000 sq. km. The Mongolian plateau is characterized by continental climate and an arid, particularly vulnerable ecosystem (Eckert et al. 2015). The Mongolian territory is divided into six natural zones: alpine, mountain taiga, forest steppe, steppe, Gobi and desert (Dash et al. 2003). The steppe zone is the largest natural zone of Mongolia which accounts for 34.2% of the total area. The steppe zone is divided into three subzones: meadow steppe, real steppe and arid steppe. Land degradation and desertification affect the whole area of the steppe zone (Dash et al. 2003). The steppe zone is defined as an arid area with precipitation lower than 250 mm per year (Dash et al. 2003). The arid area is vulnerable to changes in the climate, and human activities and land degradation processes happen more rapidly in this area (FAO and LADA 2007). The decrease in biodiversity and loss of vegetation in the Gobi and steppe zones is considered one of the main indicators of desertification. These factors make the Gobi and steppe zones more vulnerable and prone to land degradation, and human activities and climate variations can trigger further vegetation cover loss and desertification (Dash et al. 2003). For these reasons, the real steppe subzone located in the east part of Mongolia was selected for the study site.

The UNCCD definition of desertification is "*land degradation in arid, semi-arid and dry sub-humid areas resulting from various factors, including climatic variations and human activities*" (UNCCD 2013). Early detection and observation of land degradation is the main challenge of scientists and policymakers (Higginbottom & Symeonakis 2014). It is better and easier to prevent or minimize land degradation than to restore degraded and desertified land. Remote sensing methods are the main choice for the development of an environmental monitoring system because of its availability to rapid overview over large regions at relatively low cost (Higginbottom & Symeonakis 2014). The most frequently used satellite earth observation dataset is the NDVI (Normalized Difference Vegetation Index). The NDVI is the estimated result of remote sensing measurements that indicate greenness of the vegetation and patterns of green biomass (Forkel et al. 2013). The NDVI is selected as one of the biophysical indicators of land degradation assessment in arid areas (FAO & LADA 2007). Mongolian and international scientists have agreed that long-term decline of vegetation cover is a sign of desertification (Dash et al. 2003; Lantieri, as cited in FAO & LADA 2007).

Climate variation and human activities are accelerating land degradation processes and the effects are rapidly expanding in arid areas (Dash et al. 2003). Climate variation is a primary impact that affects environmental changes in the steppe zone (Dash et al. 2003). The most important climatic parameter in the land degradation assessment of drylands is precipitation (FAO & LADA 2007). Land condition and desertification impact can be estimated by comparison between NDVI series and the rainfall series (Lantieri, as cited in FAO & LADA 2007). Therefore, precipitation and NDVI data were selected as main indicators for the study. In addition to climate variations, as mentioned before human activities highly contribute to desertification. Grazing, mining, cultivation and other land conversion practised by humans are considered principal causes of land degradation and desertification (MOFA 2015). These activities intensify desertification in the dryland of Mongolia (Dash et al. 2003). Mongolia has five types of pastoral livestock: goats, sheep, cattle, horses and camels. In 2017, the total number of livestock had reached 61 million (National Statistical Office of Mongolia 2017) and this growth in livestock numbers has led to land degradation (Wang & Batkhishig 2014). Overgrazing has affected biodiversity and the loss of some indigenous species (Wang &

Batkhishig 2014). Moreover, there are large mining industries located in the dry zones of Mongolia and they impact the ecosystem of the surrounding dry areas heavily (Dash et al. 2003). This study was conducted to assessing the response of vegetative cover to human activities and to identify human activities which contributed to loss of vegetative cover.

Scientific research papers commonly review complex methods which combine statistical and ecological framework using NDVI data in the assessment of land degradation and desertification. Recently, many researchers have been using statistical analysis for NDVI time series to detect land degradation by the trend sign of NDVI and the precipitation amount. For example, Gao et al. (2013) used the Pearson correlation coefficient to predict long-term variation of NPP (net primary productive) on the Tibetan Plateau. Also, Zhang et al. (2013) and Bai & Dent (2007) used statistical analyses methods on NDVI values for assessing the decline and regeneration of vegetation cover.

This study aimed to assess land degradation and desertification using trends in NDVI and identifying the response to precipitation variance and human activities. The complex method of GIS and statistical analyses was conducted to identify trends in vegetation cover using remotely sensed NDVI and precipitation time series data from June, July and August from 2006 to 2016. Statistical and spatial analysing methods were used for estimating the linear trend in NDVI and amount of precipitation. The outcome of this study can be used to predict future trends of decline and regeneration of the vegetation cover in the study area.

1.1 Project effects and importance for land condition assessment

Assessment of land condition is the initial process of land management planning and implementing mitigation measures of land degradation. Accurate and real-time information about land condition is critical for land managers and policymakers to develop a proper policy and land management plan. Furthermore, it is important to increase awareness about desertification and land degradation among the decisionmakers and public (Institute of Geoecology, Mongolian Academy of Science 2014).

Even though land restoration measures are included in land management plans, most regions of Mongolia are affected by desertification and land degradation (MNEGDT 2012). Land management sector officials and land officers are usually facing a lack of information about the land condition. The law on land of Mongolia includes provisions for land condition assessment measures identified as "*monitoring of land quality and characteristics*" (Law on Land-Mongolia 2002). According to this legal provision, every 5 years officials organize land characteristic and quality monitoring measures. Land management actions at all administration levels have been conducted based on these land monitoring data. But determining land condition has required much cost, time and labour. Therefore, frequency and time of land degradation monitoring is long-term (5 years), and usually means state officials using outdated monitoring data for land management planning. Thus, there is a need to introduce a simpler and cost-effective method that can be used in annual land condition monitoring assessment. Remote sensing measurements can be one of the candidates for the assessment in land condition, in addition to existing monitoring measures (Higginbottom & Symeonakis 2014). The main advantage of remote sensing measurement is the possibility to analyse a large area in a short time. On the other hand, it is impossible to use remote sensing to measure some attributes of land in detail. Therefore, land officials need to develop a new complex method to assess land condition, combining field survey data and remote sensing measurements. The remote sensing

data analyses can be validated by geographic data and field surveying measurements. This study and other similar studies can contribute to developing time and cost-saving, easy, and effective land condition monitoring methods based on remotely sensed earth observation data analyses validated by field surveying and geographical data.

1.2 Goal and objectives

Overall goal: To assess land degradation and desertification using trends of NDVI time series and identifying the effects of human activities and precipitation variation.

Specific objectives:

- To estimate trends in annual average NDVI and annual average accumulated precipitation for June, July and August from 2006 to 2016.
- To identify the effects of human activities and precipitation variables on the NDVI trend.

2. METHOD OF STUDY

2.1 Study area

Location: The study area is located in the east part of Mongolia; the elevation ranges between 604 - 1,555 m above sea level and covers a total area of 21,735.9 sq. km. The site is located across the territory of Erdenetsagaan soum[1] of the Sukhbaatar aimag[2] and Matad, the Khalkhgol soum of Dornod aimag, and borders with China in the south and north, respectively. The study area belongs to the real steppe subzone of Mongolian steppe (Fig. 1 and Figure 2).

(a) (b)

Figure 1. View of real steppe subzone landscape. (a) Landscape of southern part of the study area. (b) Landscape of northern part of the study area. (Photos: (a) T. Bekhe, (b) N. Motsumoto)

[1] Mongolia has a 4-level of administration unit; Soum is the third level of administration unit, like a district.
[2] "Aimag" is the secondary level administration unit of Mongolia, like a province. An Aimag is divided into Soums.

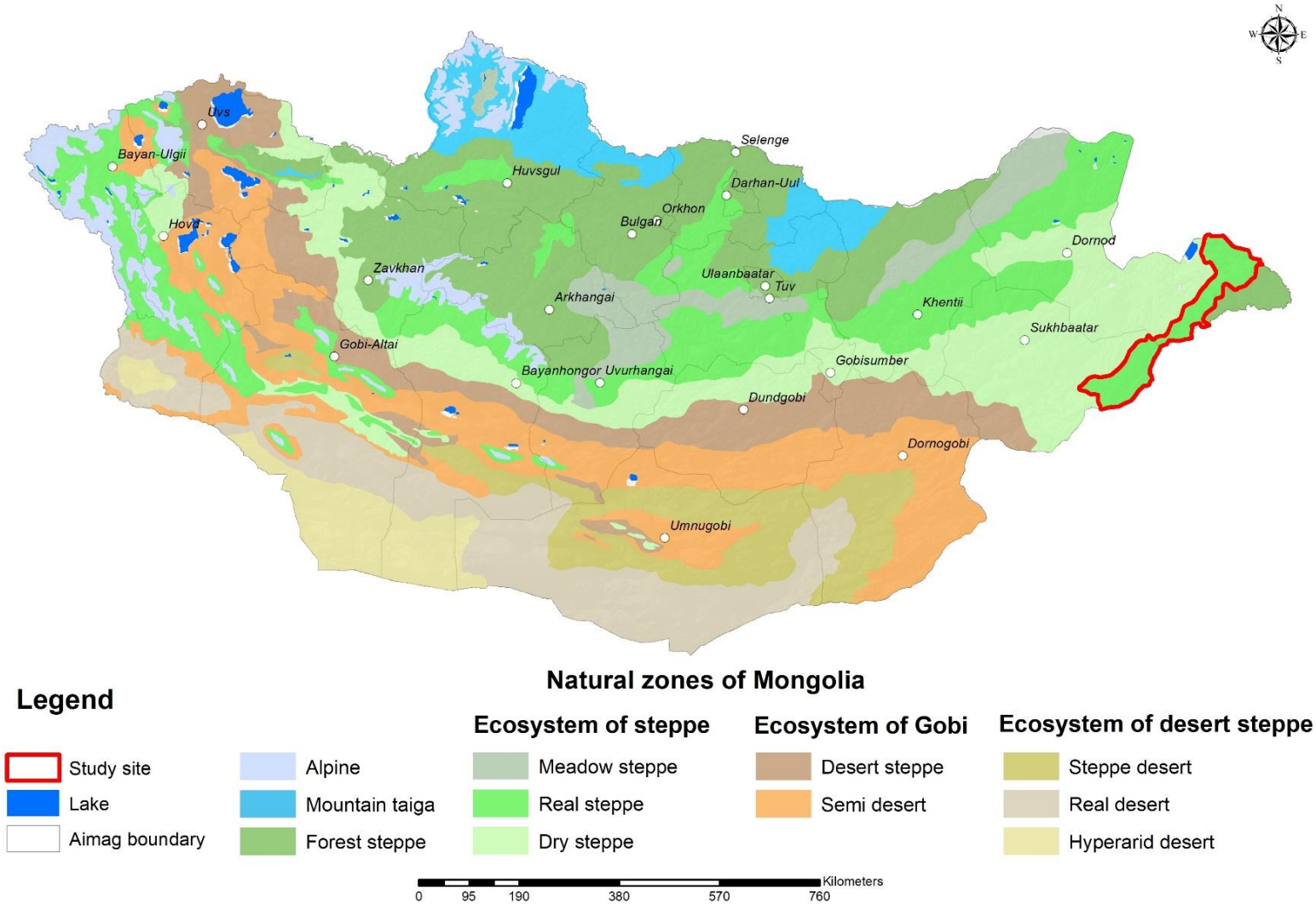

Figure 2. Mongolia is divided into six natural zones. Each natural zone is divided into different subzones according to its ecosystem features and altitude. The red line indicates the boundary of the study area.

Land use: The land use of the study area can be divided into two different sections, depending on human influence: under human influence and with no human impact. The southern part of the area is under high pressure from human activities: it has a substantial number of livestock and 14 mining sites currently under operation. In the northern part there is a small number of livestock and 45300 ha of croplands. In the middle part, there is a special protected area without any disturbance by human activities (Figure 3). These parts make the study area a unique place that allows assessment of how the human activities have affected the vegetation cover in the steppe zone. The main land use types causing pressure on the land in the study area are grazing and track roads (Figure 4). The areas under pasturing activities include areas around water points and herders' seasonal camps where a substantial number of animals crowd. Moreover, people use dirt roads in their everyday activities due to the fact there is no paved road in the study area. Dirt roads are easily broken under the effects of water and wind impact and vehicles create new tracks along the old road, resulting in the formation and expansion of the multiple dirt roads in the study area. In addition, mining activities cause the formation and expansion of dirt roads. Additionally, the special protected area located in the centre and southern part of the study area could be used as a reference area to compare areas affected by human influence.

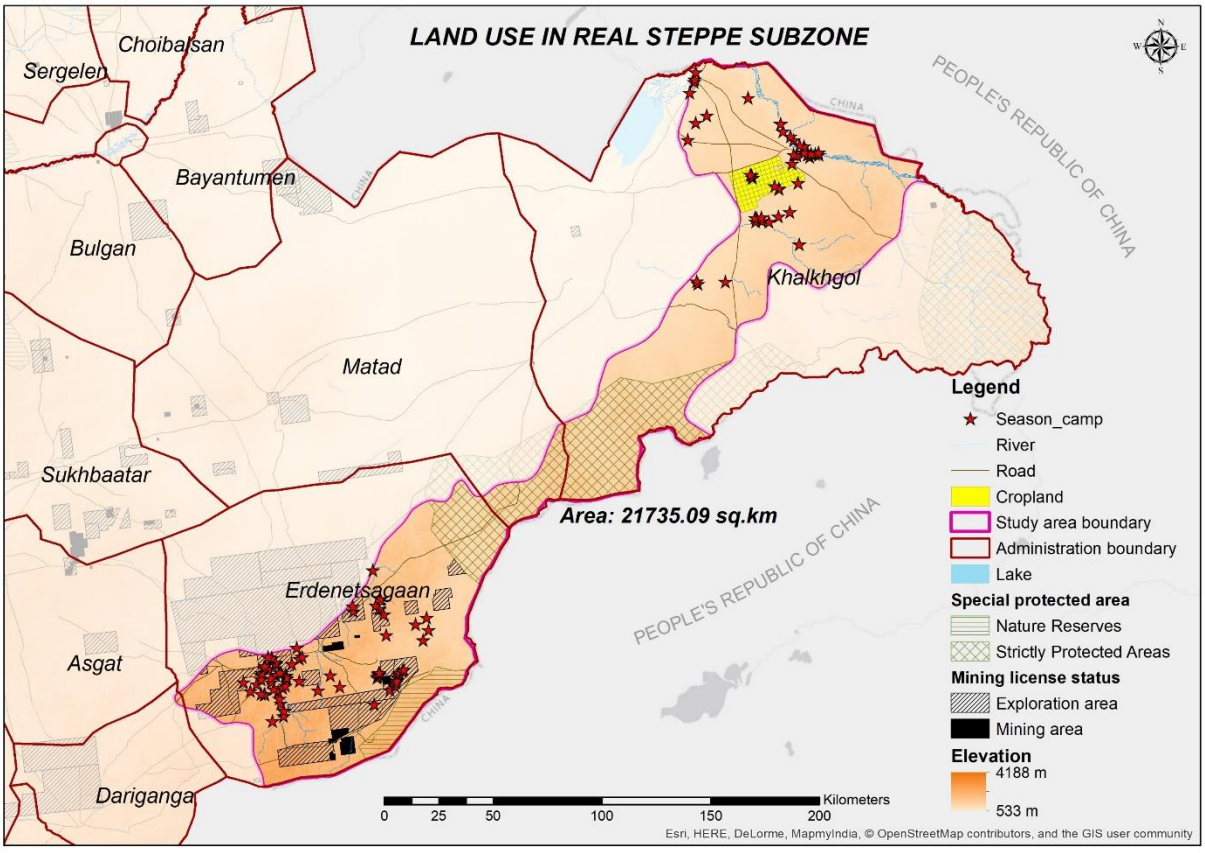

Figure 3. Land use of study area. Total area of study area is 21735.09 sq. km. The elevation of the study area gradually increases from north to south.

(a) (b)

Figure 4. (a) Land use around water points. (b) Expansion of road impact zones (Photos: (a) https://www.mofa.gov.mn/new/cache/widgetkit/gallery/40/00001891-e45241de83.jpg (b) http://resource.24tsag.mn/24tsag/photo/2013/9/845304d747af1e3e/465a9de2030ac65boriginal.jpg)

Climate features: The climate of the Mongolian steppe zone is very variable due to high variations in temperature, low precipitation and strong winds (Dash et al. 2003). The growing season in Mongolia is very short, from May to August, and the highest temperatures and highest precipitation occur from June to August (Figure 5). Figure 5 shows the Khalkhgol meteorological station's data, which is located within the study area.

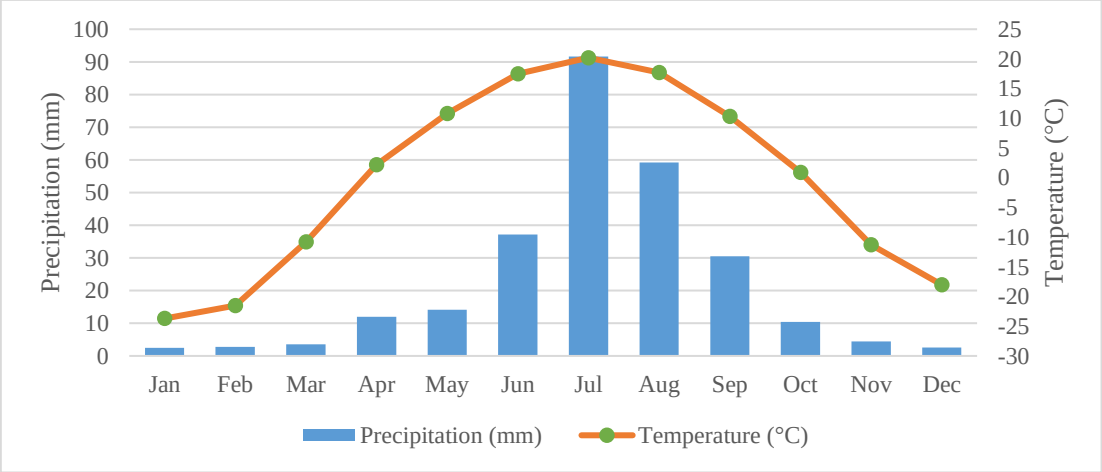

Figure 5. Monthly average precipitation and monthly average temperature of Khalkhgol soum (Data from the Mongolian National Agency for Meteorology and Environment Monitoring)

2.2 Datasets utilized

The temporal coverage of the study was 11 years from 2006 to 2016. The remotely sensed NDVI and precipitation data of June, July and August were collected for that period.

Normalized difference vegetation index (NDVI): This study analysed data from the MODIS satellite's MOD13A3 NDVI data of June, July and August for a period of 11 years. The MOD13A3 vegetation index product is the Terra MODIS version 6 NDVI dataset which referred to the continuity index from the National Oceanic and Atmospheric Administration-Advanced Very High Resolution Radiometer (NOAA-AVHRR) (Solano et al. 2010). MODIS NDVI is calculated following the formula:

$$NDVI = \frac{NIR - Red}{NIR + Red} \quad \text{(I)}$$

MOD13A3 NDVI data values range from -2000 – 10000 with a scale factor of 0.0001. The lower values (below 1000) represent water bodies, snow, barren land, rock and sand. The higher values (above 1000) represent vegetation cover such as shrubs, grasslands and forest. MOD13A3 NDVI data's spatial resolution is 1 km and the temporal resolution is monthly. MOD13A3 data are a global vegetation dataset spanning three decades (Forkel et al. 2013) which allows the use of long-term analyses of land cover in large areas (Ustin et al. 2009). This study focused on quite a large area and the MOD13A3 dataset was compatible for this study. The data are open and freely accessible from USGS's (United States Geological Survey) homepage: earthexplorer.usgs.gov (More detailed information is included in Appendix I).

Precipitation data: The distribution of the weather station network is very sparse across Mongolia. The study area is located across the territory of three soums and each soum has one weather station monitoring changes in the weather. These weather stations estimate the monthly precipitation data for the whole area of each soum, which is inadequate to generate a spatial distribution of monthly precipitation with close approximation of scale and accuracy to the NDVI dataset. In order to estimate spatial distribution of the amount of precipitation densely distributed precipitation data are needed. Therefore, remotely sensed precipitation data derived from TRMM's (Tropical rainfall measuring mission) were acquired to estimate the annual average accumulated precipitation for June, July and August from 2006 to 2016. In 1997, the TRMM mission was jointly launched by NASA (National Aeronautics Space Agency) and JAXA (Japanese Aerospace Exploration Agency) to study the climate factors of precipitation and weather. TRMM's monthly precipitation 3B43 data were collected for this study. Multi-satellite precipitation 3B43 data give the monthly precipitation estimated by the Microwave-IR gauge on a global scale combining two months starts from 1998 (Huffman 2016). The spatial resolution of this product is a 0.25^{o}x0.25^{o} grid and the temporal resolution is monthly (Huffman 2016). It presents the monthly average precipitation in mm/hour per pixel of the 0.25^{o}x0.25^{o} grid. 3B43 precipitation data can be downloaded with the format NetCDF from NASA's precipitation measurement missions (PMM) homepage: https://pmm.nasa.gov/data-access/downloads/ (More detailed information is included in Appendix I).

Vector data: The vector data include roads, settlement areas and herders' seasonal location points, wells, rivers and streams within the selected area. The data acquired were from the "National unified land territory registration" data which has been developed by the Agency of Land Administration and Land Management, Geodesy and Cartography.

2.3 Data analyses

NDVI trend analyses: Recently many scientific papers have been published related to the vegetative cover analyses, mostly used statistical analyses for estimating the trend in NDVI. There are some studies using the Pearson correlation coefficient to calculate the relationship between the NDVI variables and its time duration in a specific part of the Mongolian Plateau (Gao et al. 2013; Zhang et al. 2013). The Pearson correlation coefficient is used to measure linear relationship between two quantitative and continuous variables. In this study the Pearson correlation coefficient was used for investigating correlations between the total annual NDVI values for a selected area and the sequence of the given time *n.* Piao & Fang (2002) used the

Pearson correlation to predict the long-term trend of Net primary product (NPP), as shown in the following formula:

$$r_{xt} = \frac{\sum_{i=1}^{n}(x_i - \bar{x})(i - \bar{t})}{\sqrt{\sum_{i=1}^{n}(x_i - \bar{x})^2 \sum_{i=1}^{n}(i - \bar{t})^2}} \quad \text{(II)}$$

where *n* represents sequential year, x_i represents the NDVI value in the i^{th} year, $\bar{x}$ is the mean value of NDVI in the multiyear and $\bar{t}$ - the average value of the consecutive years equal to (n + 1)/2 (Gao et al. 2013). The result of this analysis has been shown as the estimated positive and negative values for each of the pixels (22043) that indicate an ascending and or descending linear trend within the given period.

Precipitation trend analyses: Precipitation data is analysed by the same method as the NDVI trend analysis presented above. But in this case x_i represents the average annual accumulated precipitation for June, July and August in the *i*th year, and $\bar{x}$ is the mean value of total precipitation for the multiyear (Gao et al. 2013). The result of this analysis shows the estimated positive and negative values that indicate the ascending and descending linear trend for each of the 22043 pixels of total precipitation within the given period (Gao et al. 2013). After that, calculation of the Pearson correlation coefficients were used for identifying the relationship NDVI and the rainfall time series over the 11-year period. If the correlation coefficient result is larger than 0 it represents a positive correlation and lower than 0, a negative correlation between two variables (Tong et al. 2017). Pearson correlation coefficient formula:

$$r_{xy} = \frac{\sum_{i=1}^{n}(x_i - \bar{x})(y_i - \bar{y})}{\sqrt{\sum_{i=1}^{n}(x_i - \bar{x})^2 \sum_{i=1}^{n}(y_i - \bar{y})^2}} \quad \text{(III)}$$

where r_{xy} represents the correlation of two variables *x* and *y*, x_i is the growing season NDVI of the i^{th} year, y is the precipitation time series, $\bar{x}$ and $\bar{y}$ are the mean values of NDVI and precipitation, in the growing season from 2006-2016 (Tong et al. 2017).

Human activity spatial distribution analyses: Sanderson et al. (2002) developed human influence index calculating procedures. They were created indicating spatial buffer zones from 2 to 15 km in each category of area under human influence and giving specific scores for different zones depending on distance from the objects of human influence (Sanderson et al. 2002). Moreover, Gao et al. (2013) and other researchers created 10 different buffer zones from human impact zones where the distance between each zone is 1 km. These studies and other similar studies regarding human footprints set specified sizes of buffer zones from human activities, taking into account specific characteristics of the study area and resolution of the data. In this study area there were several types of human activities and these activities can be classified into two main categories, agricultural and infrastructural activities. Agricultural activities include cropland, herder camps, lakes, water points, rivers and streams, and infrastructural activities include settlement areas, roads and mining. The buffer zones were determined by the impact zones mentioned above. In the study site, sparse distribution of population in vast areas and a relatively flat topography are characteristics that have affected human land use and livestock grazing. For example, herders herd their livestock at remote distances from their seasonal camps and they choose their camp locations near to the road and water points and rivers in summer time. Considering the above factors and the resolution of NDVI data, we created three buffer zones from human activity at the following distances: 2 km

(high impact zone), 4 km (medium impact zone) and 10 km (low impact zone) from. Only one buffer zone was created with a 1 km distance zone from cropland and the mining area depends on the specification of land use. Then we carried out overlay analyses to combine NDVI ascending and descending trend values and various human impact zones to generate the spatial distribution of NDVI trends on each human impact buffer zone (Gao et al. 2013).

2.4 Data processing

ArcGIS 10.3.1 program's Spatial analyst tools, Multidimension tools, and Conversion tools were used for the data processing. The statistical analyses were conducted in MS Excel 2016 and SAS Enterprise Guide 7.1.

NDVI data: The annual average NDVI values were calculated from the monthly NDVI MOD13A3 data for June, July and August for the period of 2006 to 2016. Then each 11-year NDVI mean values were extracted from each pixel within the study area for the 22043 points for the next analyses. The 11-year annual average NDVI trend was calculated using the Pearson correlation coefficient for each year's annual mean values for the 22043 points, using MS Excel 2016. A significance test was conducted for the correlation coefficient of the NDVI trend analyses to identify the probability value (p value). After that, spatial distributions of the NDVI trend images were generated using the spatial analyst tool.

Precipitation data: TRMM 3b43 surface precipitation data from the TRMM satellite with a 0.25^{o} grid resolution were imported using netCDF format and clipped accordingly to conform to the border study area. In order to estimate the correlation between the trend in NDVI and the precipitation amount, the spatial resolution of these two datasets should be the same. In doing so, we changed the spatial resolution of the TRMM precipitation data from a 0.25^{o} grid to 1 km, using the resample tool of the raster processing. After that, we calculated the average accumulated precipitation for the 3 months (June, July, August), using the raster calculator tool and producing its spatial distribution image. Then images were extracted for the total 22043 points to generate each year's spatial distribution map and numerical variables of the amount of precipitation. The 11-year linear trend of precipitation was calculated using the Pearson correlation coefficient formula on each year's average accumulated precipitation value of 22043 points. After that, a two-tailed significance test was conducted on the correlation coefficient of the NDVI trend analysis to identify the probability value (p value).

Vector data processing: Human influence specific buffer zones were created 2 km, 4 km and 10 km from roads, settlement areas, wells, springs, rivers and streams within the study area. The buffer zones were converted into raster format with 1 km resolution. The effect of human activities on the NDVI trend were defined through identifying the spatial distribution of the decreasing and increasing trends in the NDVI values among the human impact buffer zones with different distances of 2 km, 4 km, 10 km from the human activities using overlay analysis.

3. RESULTS

3.1 Trends in annual average NDVI

Summary statistical analyses were conducted to estimate the 11-year annual average NDVI values before analysing the multi-year trend (Appendix 2). Over the 11 years dynamic changes

in the annual average NDVI values tended to increase in given periods, but there was no significant increase or decrease in trends in any given period (Figure 6). The increasing trendline exceeds the line for the total average from the middle of the whole period (Figure 6).

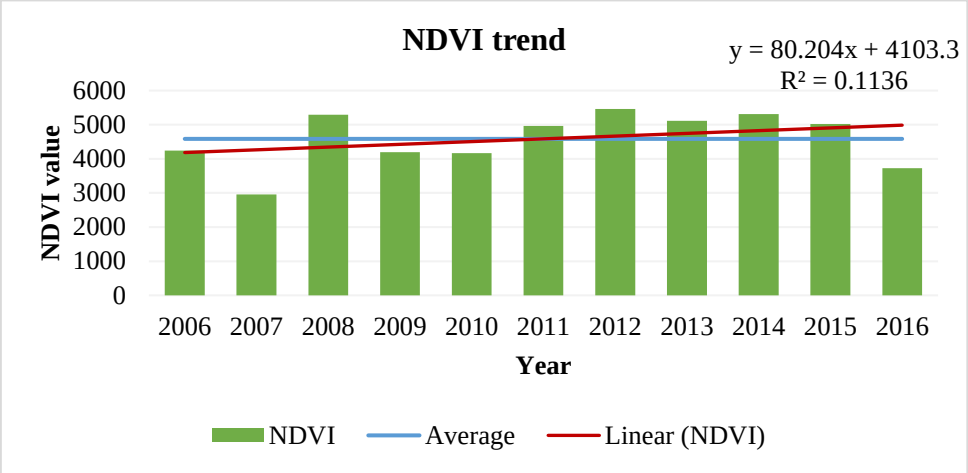

Figure 6. 11-year (2006-2016) trend in annual average NDVI for June, July and August.

Figure 7 shows the spatial distribution of the NDVI trend calculated with a Pearson correlation coefficient for the 22,043 points (x; y). Most of the increased trends were observed in the southern part, whereas the and decreased trends were mostly observed in the northern part of the study area (Figure 7). The maximum increasing trend R value was 0.86 ($p < 0.001$) (p value calculated using two-tailed T test), and the minimum decreasing trend R value was -0.54 ($p < 0.1$). The distribution of the increasing NDVI trend occupied 86.5% 18,810.52 sq. km) of the total study area and the decreasing trend 13.5% (2,923.4 sq. km) (Table 1).

Table 1. Spatial distribution percentage of NDVI trend values.

	Area (sq. km)	Percentage of total area (%)
Increasing trend	18810.52	86.54
Decreasing trend	2923.37	13.45
Total	21735.09	100.00

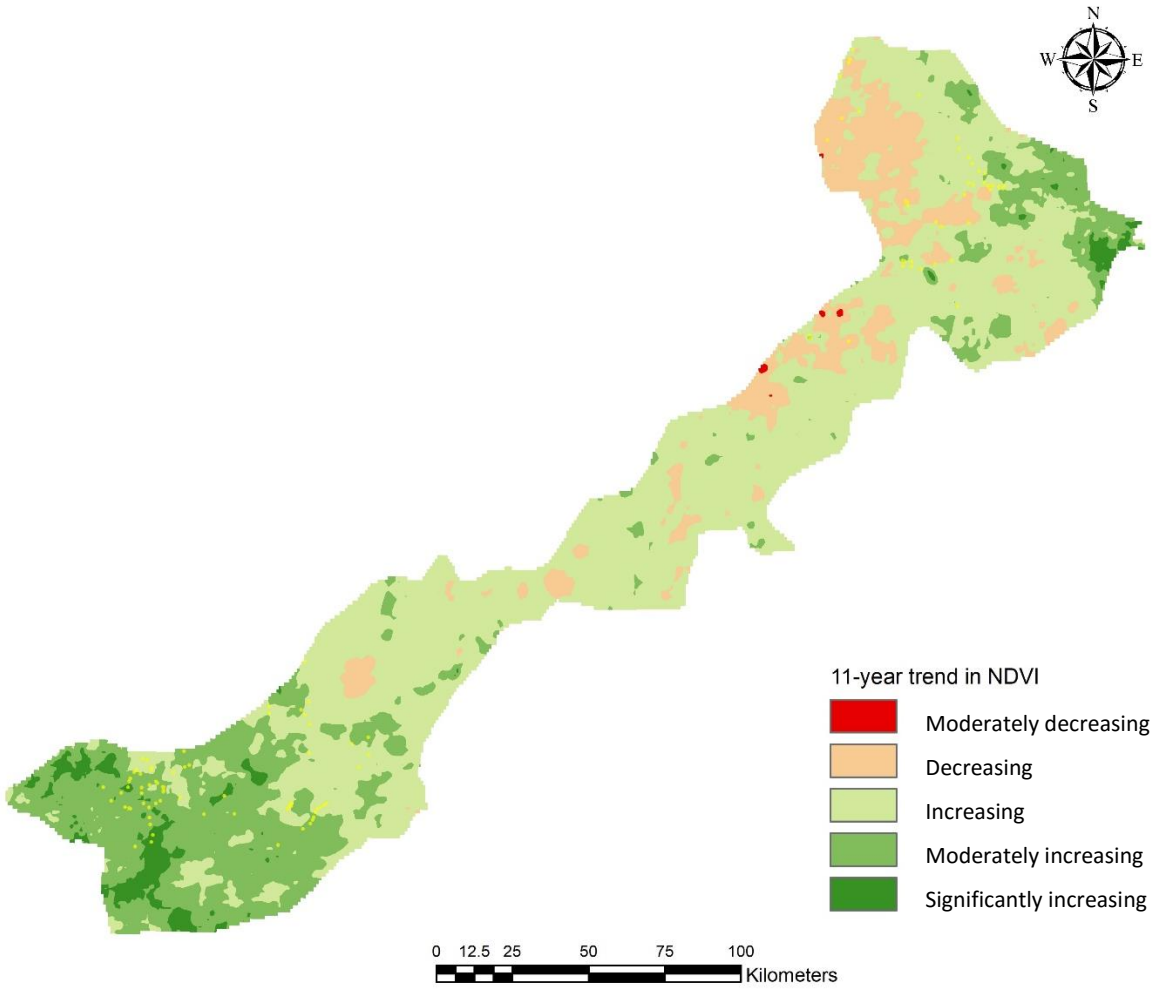

Figure 7. Pearson correlation coefficient's NDVI trend R values specified the following classes: moderately decreasing trend R value was -0.54 ($p < 0.09$) - -0.4 ($p < 0.2$), decreasing -0.4 ($p < 0.2$) – 0 ($p < 0.9$), moderately increasing 0.4 ($p > 0.2$) - 0.6 ($p > 0.05$), significantly increasing 0.6 ($p < 0.05$) - 0.83 ($p < 0.001$).

3.2 Trends in annual accumulated precipitation of study area

The 11-year annual accumulated precipitation for June, July and August was calculated before analysing for the multi-year trend (Appendix 3). As shown in Figure 8, the 11-year dynamic change average annual accumulated precipitation tended to increase in the given period. Also, there were some significant changes in the graphs which show high variance of annual accumulated precipitation in the given period (Figure 8). The increasing trendline exceeded the line for the total average from the middle of the whole period which was same result as the NDVI linear trend.

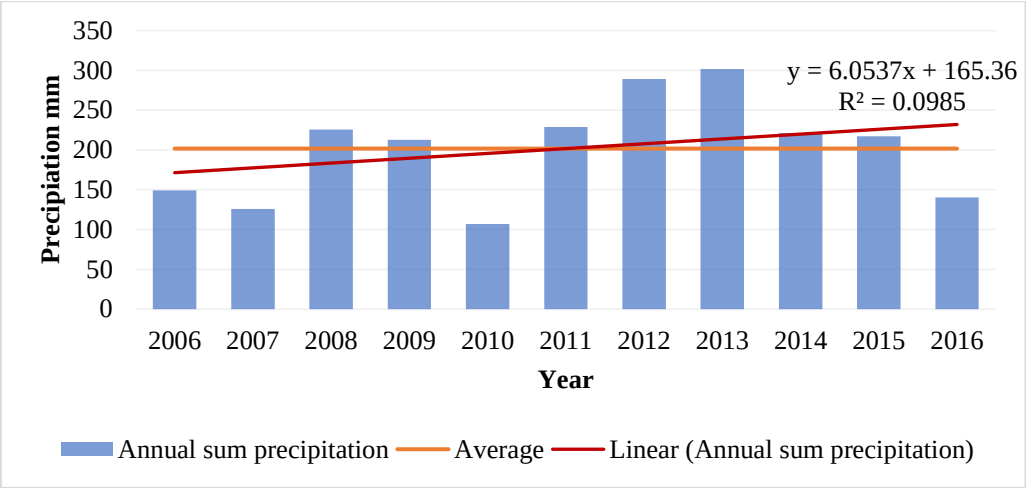

Figure 8. Dynamic change in 11-year trends in average annual accumulated precipitation for June, July and August.

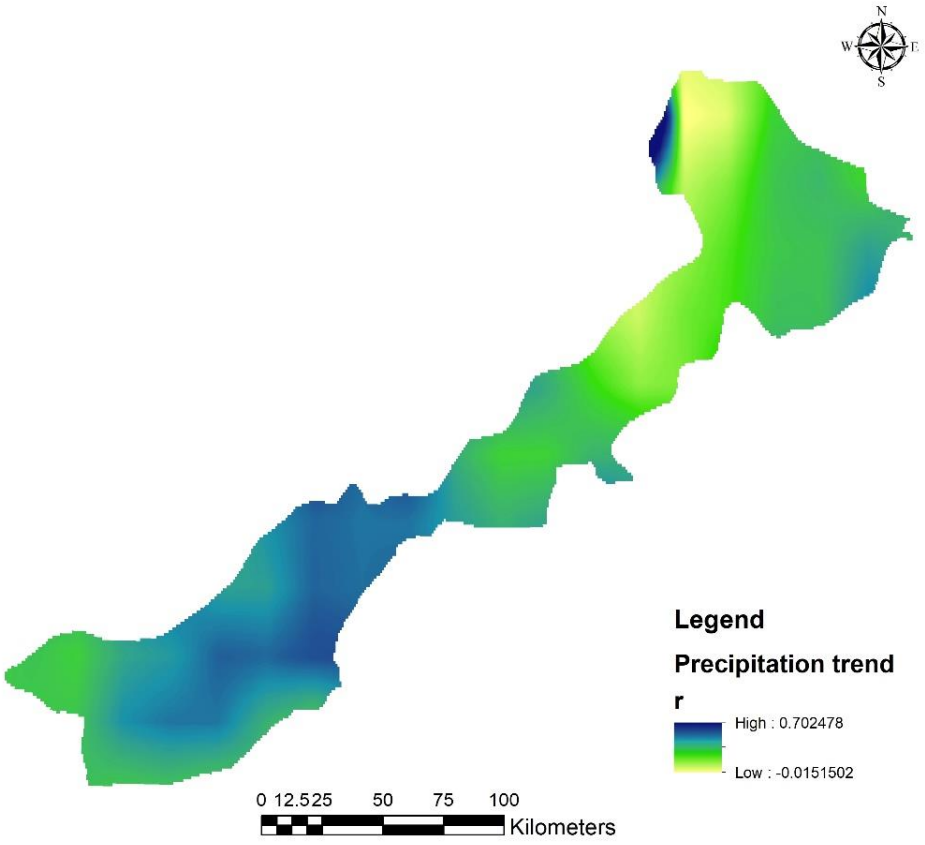

Figure 9. Spatial distribution of 11-year trends in average annual accumulated precipitation for June, July and August. The estimation result of the precipitation trend shows that 99.6% of the study area had an increasing trend and 0.4% a decreasing trend.

Figure 9 shows the spatial distribution of the precipitation trend calculated with the Pearson correlation coefficient for the 22,043 points (x; y). Precipitation in the study area tended to increase during the 11 years. The maximum increasing trend R value was 0.7 ($p < 0.001$), and the minimum decreasing trend R value was -0.01 ($p < 0.9$).

The precipitation trend had a higher variance than the NDVI variation but generally the trend variance of 2 variations looked similar over the 11-year period (Figure 10).

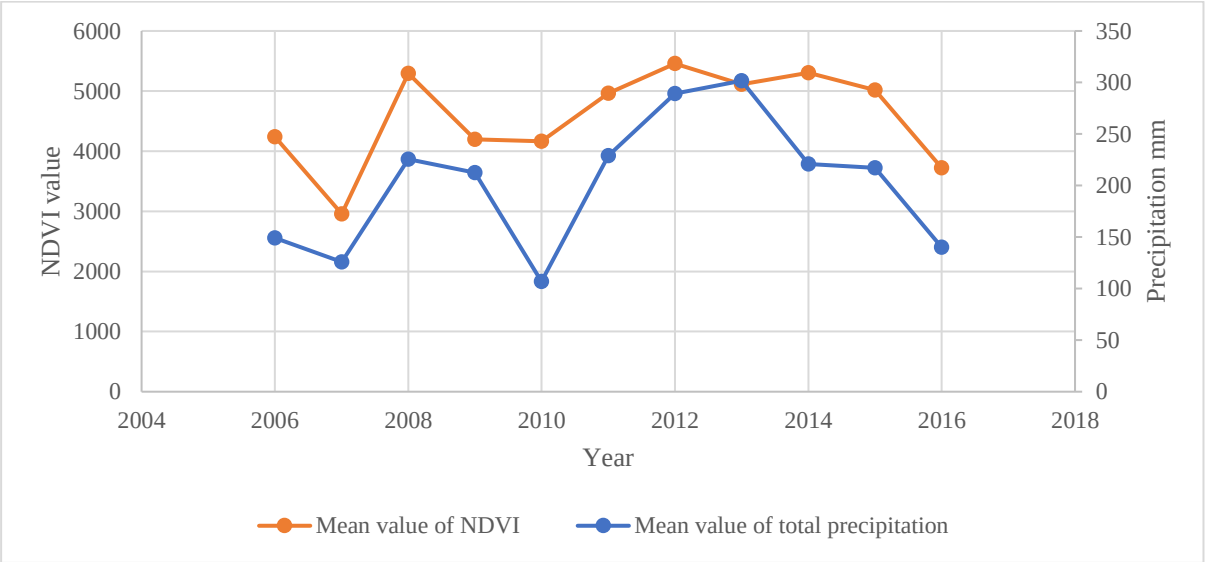

Figure 10. Comparison of annual average NDVI and annual accumulated precipitation of given period.

3.3 Spatial distribution of human activities

The spatial distribution of human impact buffer zones was created from the following human activities: herder camps, water points, lakes, rivers, settlement areas and roads (Figure 11). The total area of the study site high impact zone was 30.1% (6,542.3 sq. km), medium impact zone 22.6% (4,912.1 sq. km), low impact zone 18.9% (4,101.4 sq. km) and no impact zone 28.4% (6,177.1 sq. km).

The NDVI decreasing trend values were distributed over 16.28% of the high impact zone and 9.1% of the no impact zone (Table 2). The percentage of the area with a decreasing trend of NDVI gradually decreased from the high impact zone to the no impact zone (Figure 12).

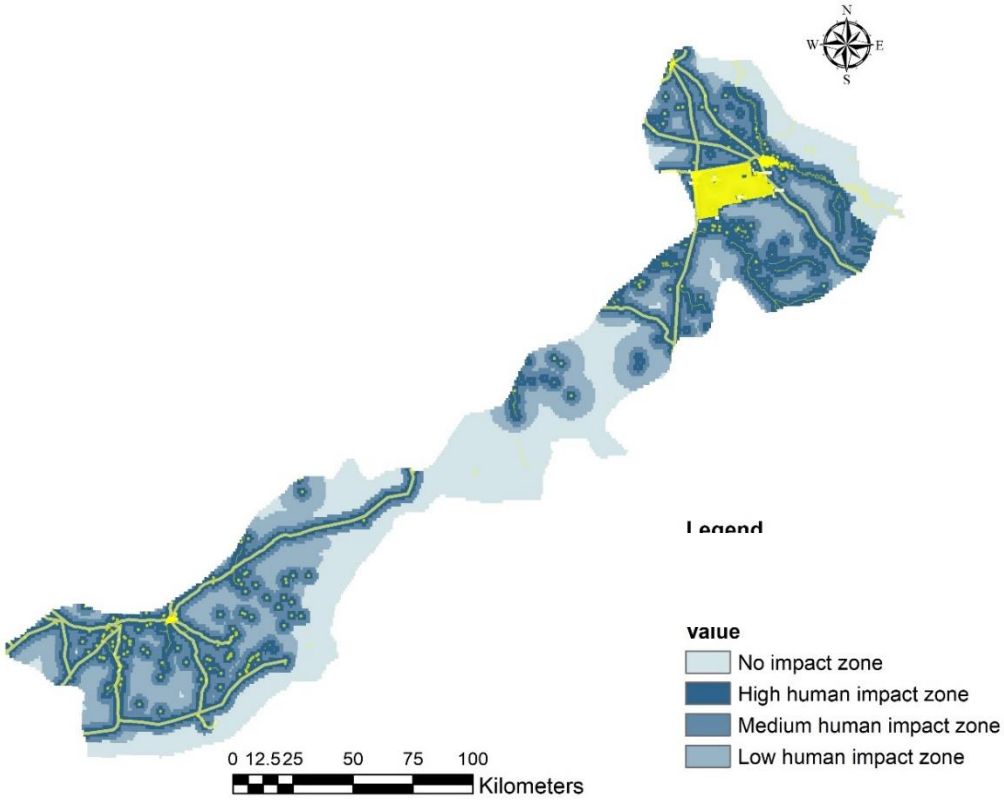

Figure 11. Spatial distribution of human impact zones classified as the following: severely 0-2 km, moderately 2-4 km, slightly 4-10 km.

Table 2. Percentage of spatial distribution of decreasing NDVI trend in human impact zones.

Human impact zone	High impact zone	Medium impact zone	Low impact zone	No impact zone
Decreasing trend %	16.28	15.79	12.69	9.09
Percentage in total study area %	30.21	22.49	18.95	28.35

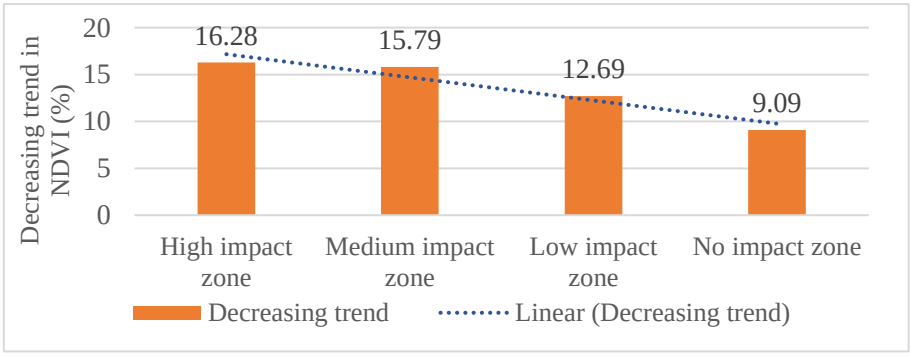

Figure 12. Percentage of spatial distribution of decreasing NDVI trend in human impact zones.

3.4 Impacts of human activities on NDVI trend

As shown in Table 3, in the impact zones from roads and settlement areas an NDVI decreasing trend was observed for 18.96% of the total area of the 2 km buffer zone, in the 4 km buffer zone 21.77% and in the 10 km buffer zone 22.81%, respectively. The impact zone of roads had more decreasing trend values than settlement areas.

Table 3. Percentage of NDVI decreasing trends in impact zones of settlement areas and roads.

Buffer zone distance (km)	2	4	10
Urban area (%)	10.26	11.54	13.33
Road area (%)	18.16	19.30	15.84
Total percentage decreasing trends	18.96	21.77	22.81

As shown in Table 4, in the impact zones from grazing activities 88.5% increased and 11.5% decreased. Overall, the increasing NDVI trend occupied 85.23% of the total grazing impact zone and the decreasing trend 17.03%.

Table 4. Percentage of spatial distribution of NDVI decreasing trends in impact zones from grazing activities.

Buffer zone distance (km)	2	4	10
Herders camp (%)	10.58	17.66	15.99
Wells and springs (%)	12.66	16.78	14.59
Rivers and streams (%)	6.65	7.58	10.45
Lakes and ponds (%)	20.48	19.78	21.58
Total percentage	11.5	15.22	15.38

In the 1 km buffer zones from cropland 32.1% of the total area had a detectable decreasing trend in NDVI (Table 5). There were no NDVI declining trends observed in the impact zones from mining activities.

Table 5. Percentage of NDVI decreasing trend distribution in the impact zones of cropland and mining activities

Other human activity factors	Cropland (1 km distance buffer)	Mining (1 km distance buffer)
Decreasing trend (%)	32.1	0.00

Figure 13 shows the percentage of values of negative trends in the total area of 1-10 km impact zone. Most of the decreasing trends observed in the area around cropland and lakes and ponds was about 20% of the total area of the impact zones.

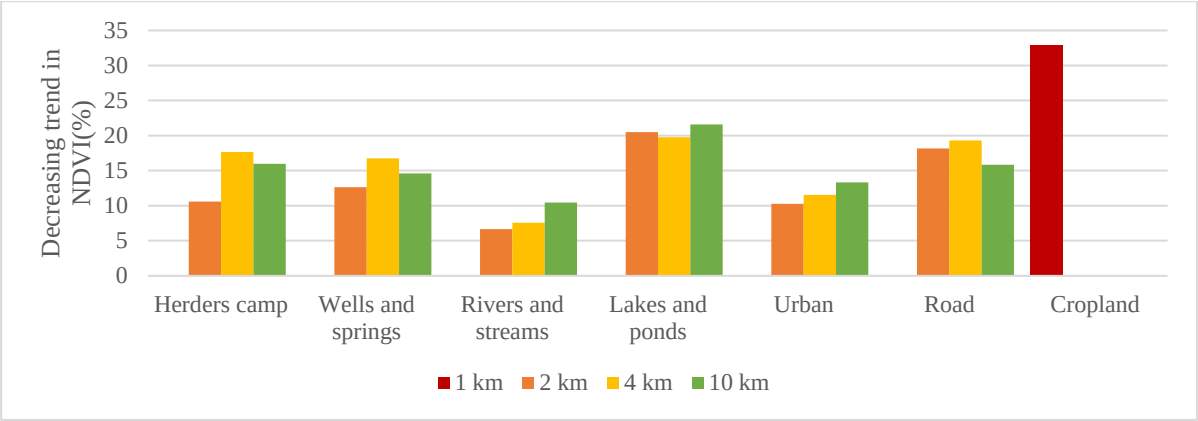

Figure 13. Percentage of decreasing trend distribution in different impact zones.

The distribution of the NDVI trend values in the no impact zones showed the following results: in natural reserves, 100% increasing trend; strictly protected areas, increasing trend 89.63% and decreasing trend 10.37%; borderline areas, increasing trend 93.92%, decreasing trend 6.08% (Table 6).

Table 6. NDVI trend in the no human influence zones

State special needs areas	Natural reserves (area: 3911.72 sq.km)	Strictly protected areas (area: 572.02 sq.km)	Borderline areas (area: 6279.67 sq.km)
Decreasing trend (%)	0	10.4	6.1

3.5 Effects of precipitation and human activity on NDVI trends

Correlation coefficients were calculated for the NDVI trends, precipitation trend and human impact zones to identify the effects of precipitation and human activities on the NDVI trend. The spatial distribution of the NDVI trend, precipitation trend and index of human impact zones was used for calculating the correlation matrix (Table 7). As shown in the correlation matrix, the spatial distribution of the NDVI trend was positive and moderately correlated with the spatial distribution of the precipitation trend and positive but weakly correlated with the spatial distribution of human activities.

Figure 14 shows the distribution of correlation coefficients for NDVI and precipitation (for June, July and August) from 2006 to 2016. Most of the strong positive correlation R values were 0.94 ($p < 0.001$), the lowest R value -0.38 ($p < 0.2$).

Table 7. Correlation matrix of three variables.

Parameter	Trend of NDVI	Trend of precipitation	Human influence
Trend of NDVI	1	0.35	0.05
Trend of precipitation	0.35	1	0.06
Human influence	0.05	0.06	1

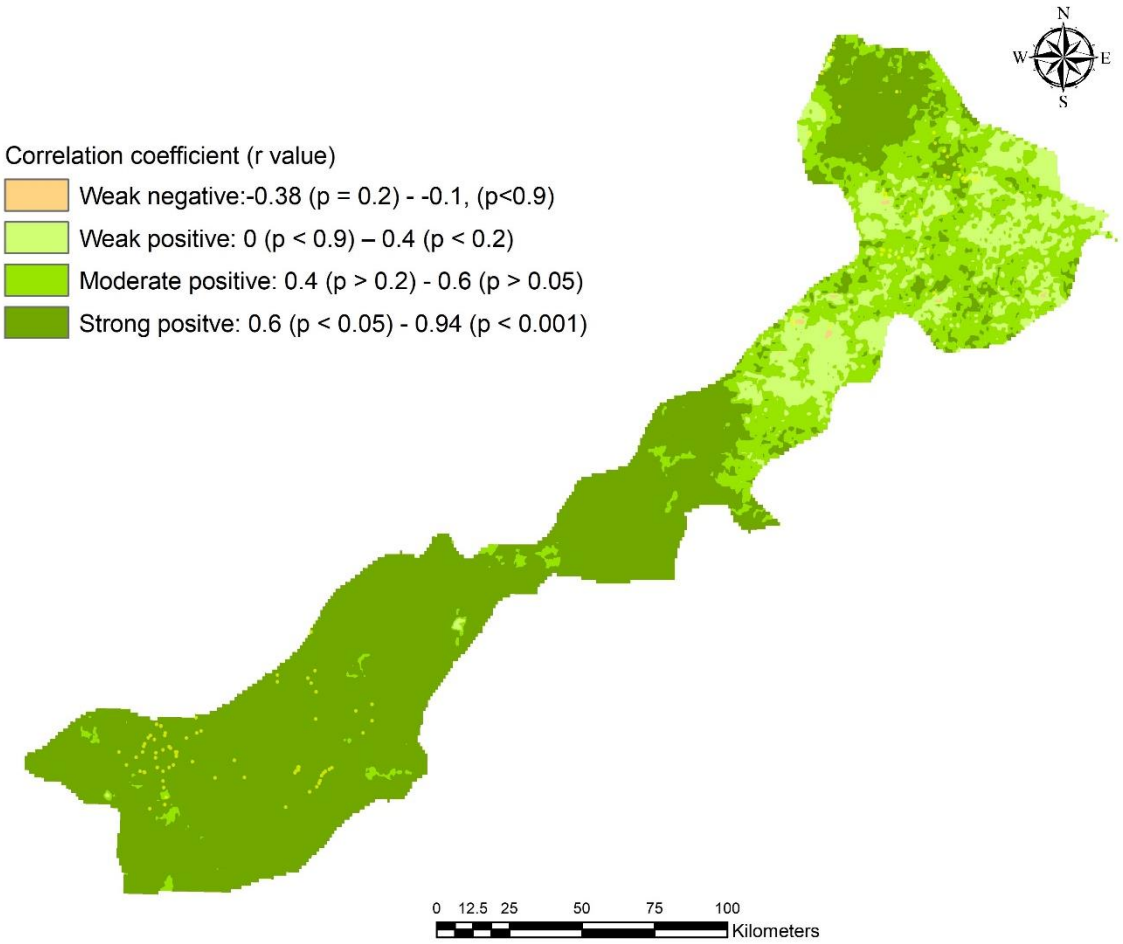

Figure 14. Correlation coefficient of annual average NDVI and annual accumulated precipitation (for June, July and August) from 2006 to 2016. Correlation coefficient of NDVI and Precipitation R values specified the following classes: weak negative R value was above -0.38 ($p = 0.2$) to -0.1, weak positive 0 ($p < 0.9$) – 0.4 ($p < 0.2$), moderate positive 0.4 ($p > 0.2$) - 0.6 ($p > 0.05$), strong positive 0.6 ($p < 0.05$) - 0.94 ($p < 0.001$).

4. DISCUSSION

The spatial distribution of the NDVI trend shows that in 11-year period 13.5% of the total area has a decreasing trend. The vegetation cover decline for the long term is defined as a sign of desertification (Lantieri, as cited in FAO and LADA 2007); it can therefore be concluded that 13.5% (2,923.4 sq. km area) of the total study area was affected by the potential impact of desertification. A significant negative trend was not detected in the study area, only a weak and moderately negative trend -0.54 ($p < 0.09$) – -0.1 ($p < 0.9$) was detected for the given period.

The variations in the average annual NDVI values and average annual accumulated precipitation trend results show similar dispersion (Figure 10). Land condition and desertification impact can be estimated by comparison between NDVI series and the rainfall series (FAO and LADA 2007). The correlation matrix revealed that the spatial distribution of NDVI trend was moderately positive ($R=0.35$, $p<0.001$) correlated with the spatial distribution of the precipitation trend and weakly positive ($R=0.05$, $p<0.001$) correlated with the spatial

distribution of human activities. But the map of the spatial distribution of the correlation coefficients between annual average NDVI and annual accumulated precipitation in the given period revealed a different result. For example, a strong correlation ($R>0.6$, $p<0.05$) was observed for most of the study area, especially in the south and centre parts, and weak and moderate correlations were observed in the northern part (Figure 14). Other factors influencing changes in the vegetation cover besides precipitation, such as human activities, strong winds and temperature variations, occurred in the areas where weak and moderate correlations were observed. Also, in the area where a strong positive correlation was observed, vegetation cover change was highly dependent on variation in precipitation. Overall, both comparison results prove that there is an obvious correlation between spatial distribution of the NDVI trend and the precipitation trend. The climate variation is a primary impact that affects environmental changes in the Arid steppe zone of Mongolia (Dash et al. 2003).

The vegetation cover has been changed variously, depending on the different land use types. Vegetation cover decline mostly occurred within the areas around lakes and croplands in the study area. The "State special needs" area was chosen as representative of the no impact zons to compare an active human impact zone with and a no impact zone. In the "State special needs" area the lowest NDVI decreasing trend was observed. In detail, the natural reserved area increasing trend accounted for 100% of the area and 89.6% of the special protected area. In the overall result, the highest percentage (16.3%) of the NDVI decreasing trend was observed in the high impact zone and the lowest percentage (9.1%) of the decreasing trend was observed in the no impact zone. The results of this comparison revealed the percentage of the decreasing trend gradually decreasing from the high impact zone to the no impact zone, which shows that human activities can affect vegetation and lead to changes in vegetative cover in different ways.

Climate variation and human activities are accelerating land degradation processes and the effects are rapidly increasing in arid areas (Dash et al. 2003). The significantly increasing precipitation trend observed in the north-western part of the study area may be because of the influence of the big lake (Buir) near to this area (Figure 9). The combined effects of human activities and precipitation variations are affecting the vegetation cover in the steppe zones. The precipitation factor appears to be affecting the decline of the vegetation cover more than human activity, according to the results of this study. In addition to precipitation, strong winds and high variation in temperature are major climatic factors impacting land degradation and the fragile ecosystem of the steppe zone (Dash et al. 2003). These climatic factors need to be considered in further studies on land degradation.

4.1 Limitations

Despite promising results there are some limitations to the datasets that were used in this research and the methodologies applied. Remotely sensed data have a common limitation concerning atmospheric, clouds, anisotropic and spectral effects which affect the quality of the results. For this study, the geometric resolution of MODIS NDVI data also influenced the accuracy of the study. Especially, NDVI data resolution was partially coarse to identify NDVI changes around small objects such as settlement areas and herder camps. A total of 320 meteorological stations are currently under operation in Mongolia. But in the study area, there are only two meteorological stations in existence which is insufficient to interpolate spatial distribution of rainfall in such a large area. TRMM's multi-satellite monthly data provided the availability to generate spatial distribution of the amount of precipitation. However, in estimating the relationship between rainfall and NDVI data, there may be errors caused by

spatial resolution differences. The method of this study was not able to fully represent total impacts which caused land degradation and desertification in the steppe area. In the steppe zone, there are various impacts which affect the change in vegetative cover, such as a wind speed and temperature variation. Also, the NDVI is a remotely sensed measurement of visible green patches of vegetation rather than an absolute indicator of vegetation biomass. Thus, further studies still need to use proper indicators capable of indicating plant biomass such as climatic factors, NDVI, EVI (Enhanced vegetation index) and NPP (Net primary productivity). The methodology of this study can be used to identify trends in any remotely sensed biophysical indicators of land degradation using any scale of time series dataset. Additionally, it is possible to conduct analyses using time series data of NDVI and rainfall which cover the entire year period to identify changes in other seasons.

5. CONCLUSIONS

The study was aimed to identify effects of precipitation variation and human activities on the decline of vegetative cover. Pearson correlation analysis was used to identify the linear trend of precipitation and NDVI variance over the 11-year period from 2006 to 2016. The dispersion of decreasing trend values of NDVI occupies 13.5% of the study area which means that for the 2,923.4 sq. km area there is the potential impact of land degradation. The percentage of decreasing trend in NDVI among the human impact zones showed that there has been a certain impact of human activity on the change in vegetation cover. The precipitation variance has moderately and human activities weakly affected the vegetation cover change. In the south and centre part of the study area the precipitation factor dominated the vegetation cover change. In the north part of the research area weak and moderate correlation was observed. This means there are more factors which affect the vegetation cover change. The variation in precipitation leads to increased vulnerability of the steppe zone to desertification. Both factors have their own effects on the decline of the NDVI trend, but the precipitation factor has a larger impact than human activities on the change of vegetation cover of the real steppe subzone. For further development of the methodology it is necessary to consider more biophysical indicators of plant biomass, and also other climatic and topographic parameters, and to prolong the observation period and increase the accuracy of the dataset. Overall this method gives opportunity to conduct a relatively quick estimation of the situation in a large area. Also, this method is suitable to identify regions where land degradation is a considerable problem.

ACKNOWLEDGEMENTS

I would like to express my special thanks of gratitude to my supervisors, Atli Gudjónsson and Ingibjörg Jónsdóttir, who provided me with professional guidance and dedicated support to successfully complete my project.

I would like to express my gratitude to the UNU-LRT Director and staff for their kind support for carrying out this project and assistance during this programme. Also thanks to the all lecturers, those who shared with us valuable knowledge and experience.

My sincere thanks go to my dearest and beloved wife, Narantsatsral.Ts, who unceasingly encouraged and inspired me to attend this programme.

I also would like to thank my directors and colleagues at the Agency for Land Administration and Management, Geodesy and Cartography, and I appreciate your support and kindness.

Finally, many thanks to the UNU-LRT 2017 fellows and my friends for your cordial relationship and fruitful collaboration.

LITERATURE CITED

Dash D, Jalbaa K, Khaulanbek A, Mandakh N (2003) Говь хээрийн бүсийн экосистемийг нөхөн сэргээх, хамгаалах шинжлэх ухааны үндэслэл [Sceintific basis of restoring and protectting ecosystem of the Gobi and Steppe zones]. http://www.eic.mn/DLDbase/upload/2012/tadesertbook/3/20121220_6190_3.pdf (accessed 14 July 2017) (in Mongolian).

Eckert S, Hüsler F, Liniger H, Hodel E (2015) Trend analysis of MODIS NDVI time series for detecting land degradation and regeneration in Mongolia. *Journal of Arid Environments* 113:16–28

FAO, LADA (2007) Technical Report 2, Biophysical indicator toolbox (Pressure/State). http://projects.inweh.unu.edu/kmland/display.php?ID=226&DISPOP=VRCPR (accessed 1 July 2017).

Forkel M, Carvalhais N, Verbesselt J, Mahecha MD, Neigh CSR, Reichstein M (2013) Trend change detection in NDVI time series: Effects of inter-annual variability and methodology. *Remote Sensing* 5:2113–2144.

Gao Q, Wan Y, Li Y, Guo Y, Ganjurjav, Qin X, Jiangcun W, Wang B (2013) Effects of topography and human activity on the net primary productivity (NPP) of alpine grassland in northern Tibet from 1981 to 2004. *International Journal of Remote Sensing* 34:2057–2069.

Higginbottom T, Symeonakis E (2014) Assessing land degradation and desertification using vegetation index data: Current frameworks and future directions. *Remote Sensing* 6:9552–9575.

Huffman GJ (2016) The Transition in Multi-Satellite products from TRMM to GPM (TMPA to IMERG). https://pmm.nasa.gov/sites/default/files/document_files/TMPA-to-IMERG_transition.pdf (accessed 9 July 2017).

Institude of Geoecology, Mongolian Academy of Science (2014) Цөлжилтийг сааруулах технологи боловсруулж турших [Core Technology Project Report on desertification reduction technology development and experiment]. http://www.eic.mn/DLDbase/upload/2016/tadesertbook/3/20160603_124_3.pdf (accessed 9 July 2017) (in Mongolian).

Law on Land Mongolia (2002) http://www.legalinfo.mn/law/details/216 (accessed 6 June 2017) (in Mongolian).

MNEGDT (Ministry of Nature, Environment, Green Development and Tourism) (2012) Байгаль орчны төлөв байдлын тайлан 2014-2015 [Environmental perspective report 2014-2015]. http://www.eic.mn/DLDbase/upload/2015/tadesertbook/4/20150616_6685_4.pdf (accessed 9 July 2017) (in Mongolian).

MOFA (Ministry of food and agriculture of Mongolia) (2015) *National Report on the Rangeland Health of Mongolia*. https://jornada.nmsu.edu/files/Mongolia-Rangeland-health-Report_EN.pdf (accessed 9 July 2017).

National statistical office of Mongolia (2017) *Monthly Statistical Report of Mongolia.* http://www.1212.mn/statHtml/statHtml.do?orgId=976&tblId=DT_NSO_1001_021V1&conn_path=I2&language=en (accessed 9 July 2017).

Piao S, Fang J (2002) Terrestrial net primary production and its spatio-temporal patterns in Qinghai-Xizang Plateau, China during 1982-1999. Journal of Natural Resources 17:373—380.

Sanderson EW, Jaiteh M, Levy MA, Redford KH, Wannebo A V, Woolmer G (2002) The human footprint and the last of the wild. *BioScience* 52:891.

Solano R, Didan K, Jacobson A, Huete A (2010) *MODIS Vegetation Index User's Guide* (MOD13 Series). The University of Arizona 2010:38.

Tong S, Zhang J, Bao Y, Wurina, Terigele, Weilisi, Lianxiao (2017) Spatial and temporal variations of vegetation cover and the relationships with climate factors in Inner Mongolia based on GIMMS NDVI3g data. *Journal of Arid Land* 9:394–407.

UNCCD (2013) Desertification a visual synthesis. http://www.unccd.int/Lists/SiteDocumentLibrary/Publications/Desertification-EN.pdf (accessed 1 July 2017).

Ustin S, Jacquemoud S, Palacios-Orueta1 A, Li L, Whiting M (2009) Remote sensing based assessment of biophysical indicators for land degradation and desertification. Pp. 15–44. In: Roeder A and Hill J (eds.) *Recent Advances in Remote Sensing and Geoinformation Processing for Land Degradation Assessment*. CRC Press, London.

Wang Q, Batkhishig O (2014) Impact of overgrazing on semiarid ecosystem soil properties: A Case study of the eastern Hovsgol lake area, Mongolia. *Ecosystem & Ecography* 4:1–7.

Zhang X, Lu X, Wang X (2013) Spatial-temporal NDVI variation of different alpine grassland classes and groups in Northern Tibet from 2000 to 2013. *Mountain Research and Development* 35:254–263.

APPENDICES

Appendix I. Detailed information from remotely sensed NDVI, precipitation data and vector data.

Dataset name	Definition	Source	Temporal coverage	Type	Spatial resolution	Temporal resolution	Scale factor & unit
MODIS satellite's MOD13A3 NDVI	Monthly average vegetation index data	MODIS Normalized Difference Vegetation Index (NDVI) complements NOAA's (National oceanic and atmospheric administration) Advanced Very High-Resolution Radiometer (AVHRR) NDVI products homepage: earthexplorer.usgs.gov	Monthly NDVI data of June, July and August in period from 2006-2016.	HDF	1km	monthly	0.0001
TRMM's (Tropical rainfall measuring mission) multi satellite's 3b43 data	Monthly average precipitation amount	TRMM mission was jointly launched by NASA (National aeronautics space agency) and JAXA (Japanese aerospace exploration agency) USGS's (United States geological survey) homepage: https://pmm.nasa.gov/data-access/downloads/trmm	Monthly precipitation data of June, July and August in period from 2006-2016.	NetCDF	0.25°x0.25° grid	monthly	mm/hour
Unified land territory registration data	Land use data. (Herders seasonal location, well, river, stream, spring, road, urban area etc.)	ALAGAC (Agency of Land administration, geodesy and cartography)	2012	shp (Shape file)	1:100 000		

Appendix II. Statistical summary test of 22,043 points showing mean, maximum, minimum value and, standard deviation and standard error of 11-year (2006-2016) annual average value of NDVI variables of June, July and August in study area.

Year	Mean	Std Dev	Std Error	Minimum	Maximum
2006	4240.98	1064.96	7.17	1877	8661
2007	2958.37	901.46	6.07	1452	7482
2008	5291.42	836.91	5.64	2409	8261
2009	4194.74	872.15	5.87	1838	7789
2010	4162.72	1020.8	6.88	1862	7873
2011	4964.84	600.19	4.04	2667	7794
2012	5456.67	739.77	4.98	1999	8562
2013	5112.96	790.3	5.32	2484	8403
2014	5307.07	703.89	4.74	2148	8289
2015	5018.59	762.72	5.14	278	8492
2016	3721.83	964.67	6.5	1684	8266

Appendix III. Statistical summary of total 22043 points showing mean, maximum, minimum value and standard deviation and standard error of 11-year (2006-2016) annual accumulated total precipitation during June, July and August in study area.

Year	Mean (mm)	Std Dev	Std Error	Minimum (mm)	Maximum (mm)
2006	149.29	26.3	0.18	91.44	265.53
2007	125.94	61.26	0.41	57.1	307.45
2008	225.61	29.48	0.2	179.54	420.3
2009	212.66	46.52	0.31	141.37	395.66
2010	106.94	29.39	0.2	69.77	276.1
2011	228.93	54.56	0.37	154.14	390.33
2012	289.13	31.58	0.21	193.67	484.1
2013	301.67	66.03	0.44	204.76	556.31
2014	220.99	44.47	0.3	168.12	490.08
2015	217.08	39.77	0.27	145.21	486.73
2016	140.29	26.69	0.18	87.09	407.54